Environ. Sci. Technol. **2007**, *41,* 5693−5700

Insight into Methyl *tert*-Butyl Ether (MTBE) Stable Isotope Fractionation from Abiotic Reference Experiments

MARTIN ELSNER,* JENNIFER MCKELVIE, GEORGES LACRAMPE COULOUME, AND BARBARA SHERWOOD LOLLAR

Stable Isotope Laboratory, University of Toronto, 22 Russell Street, Toronto, Ontario M5S 3B1, Canada

Methyl group oxidation, S_N2-type hydrolysis, and S_N1-type hydrolysis are suggested as natural transformation mechanisms of MTBE. This study reports for the first time MTBE isotopic fractionation during acid hydrolysis and for oxidation by permanganate. In acid hydrolysis, MTBE isotopic enrichment factors were $\epsilon_C = -4.9‰ \pm 0.6‰$ for carbon and $\epsilon_H = -55‰ \pm 7‰$ for hydrogen. Position-specific values were $\epsilon_{C,\text{reactive position}} = -24.3‰ \pm 2.3‰$ and $\epsilon_{H,\text{reactive position}} = -73‰ \pm 9‰$, giving kinetic isotope effects $KIE_C = 1.025 \pm 0.003$ and $KIE_H = 1.08 \pm 0.01$ consistent with an S_N1-type hydrolysis involving the *tert*-butyl group. The characteristic slope of $\Delta\delta^2H_{bulk}/\Delta\delta^{13}C_{bulk} \approx \epsilon_{bulk,H}/\epsilon_{bulk,C} = 11.1 \pm 1.3$ suggests it may identify S_N1-type hydrolysis also in settings where the pathway is not well constrained. Oxidation by permanganate was found to involve specifically the methyl group of MTBE, similar to aerobic biodegradation. Large hydrogen enrichment factors of $\epsilon_H = -109‰ \pm 9‰$ and $\epsilon_{H,\text{reactive position}} = -342‰ \pm 16‰$ indicate both large primary and large secondary hydrogen isotope effects. Significantly smaller values reported previously for aerobic biodegradation suggest that intrinsic fractionation is often masked by additional non-fractionating steps. For conservative estimates of biodegradation at field sites, the largest ϵ values reported should, therefore, be used.

Introduction

The gasoline additive methyl *tert*-butyl ether (MTBE) is one of the organic chemicals with the highest production volume worldwide (*1*), and it is one of the most frequently detected groundwater contaminants (*2*). Owing to its low sorption to organic material ($\log K_{OC} = 1.05$, (*3*)) MTBE is transported almost without retardation in aquifers, and, in the absence of biotransformation, can form large contaminant plumes (*4*). Using concentration measurements alone, unequivocal determination of MTBE biodegradation was not possible even at a site with well-known hydrogeology, a dense network of sampling wells, and an observation period of 8 years (*5*). Such information, however, is much warranted. On the one hand, natural attenuation of MTBE potentially provides an attractive sink of this compound in the environment. On the other hand, as illustrated in Scheme 1, all known transformation pathways do not directly lead to mineralization, but intermittently form the more problematic product *tert*-butyl alcohol (TBA), which may be further degraded under oxic conditions, whereas under anoxic conditions it is reported to be more persistent (*6*). Compound-specific isotope analysis (CSIA) has therefore received much attention as a new, alternative method to detect and even to quantify in-situ biodegradation of MTBE (*7*). This approach relies on measuring the compound's stable isotope ratios (i.e., $^{13}C/^{12}C$ and $^2H/^1H$ within MTBE) by gas chromatograph−isotope ratio mass spectrometry (GC−IRMS). Pronounced kinetic isotope effects (KIEs) have been observed in chemical and biochemical degradation reactions since molecules with heavy isotopes in their reactive position(s) react more slowly than molecules containing only light isotopes. Specifically, isotopic enrichment in ^{13}C in the remaining contaminant is strongest for molecules that contain the heavy isotope directly in the reacting bond (primary kinetic isotope effect) or at an adjacent bond (secondary kinetic isotope effect), whereas molecules with heavy isotopes at some distant position are not discriminated against (*8*).

These changes in stable isotope ratios—either over time in laboratory degradation studies or over distance at field sites—have the potential to deconvolve concentration changes due to transformation, from concentration changes due to other processes of mass loss. This is because relative to the large isotope fractionation identified for abiotic and biotic degradation of many organic contaminants, studies to date investigating isotope fractionation during processes such as volatilization (*9*−*11*); dissolution (*10*, *12*−*14*); diffusion (*14*, *15*); and sorption (*16*−*19*) showed either only small or no significant fractionation outside of the analytical uncertainty typical for CSIA (±0.5‰ for carbon; ±5‰ for hydrogen). While there is potential for fractionation to be more significant for δ^2H, in the case of both elements $\delta^{13}C$ and δ^2H large fractionation effects are typically only seen at a low fraction remaining, i.e., for instance where >95% sorption has occurred, or >95% vaporization (*18*, *20*). In a recent study documenting carbon isotope fractionation due to diffusion, Bouchard (*15*) also demonstrated that even in the unsaturated zone where diffusive isotope effects might be expected to be most pronounced compared to the saturated zone, such effects were only observable if measured within a few days of the spill, and where measurements could be done at a very fine spatial scale. Wang et al. (*20*) noted that while fractionation due to non-degradative processes might be relevant in cases such as remediation by air sparging, such large isotopic shifts are likely insignificant in most natural systems where comparably extensive mass loss due to volatilization or sorption is unusual. Similarly, while Prinzhofer and Pernaton (*21*) published evidence for diffusive fractionation of CH_4 isotope signatures in laboratory studies at short spatial and temporal scales, such effects have not turned out to be a significant phenomenon at field scale.

In contrast, isotope fractionation was pronounced in both aerobic and anaerobic degradation of MTBE, and the observable enrichment of heavy isotopes in the remaining contaminant molecules was successfully modeled according to the Rayleigh equation (*22*, *23*), giving in the case of carbon isotopes

* Corresponding author e-mail: martin.elsner@gsf.de; present address: Institute of Groundwater Ecology, GSF- National Research Center for Environment and Health, Ingolstädter Landstrasse 1, D-85764 Neuherberg, Germany.

10.1021/es070531o CCC: $37.00
Published on Web 07/07/2007

$$\frac{R}{R_0} = \frac{(1000 + \delta^{13}C)}{(1000 + \delta^{13}C_0)} = \frac{(1000 + \delta^{13}C_0 + \Delta\delta^{13}C_{bulk})}{(1000 + \delta^{13}C_0)} \cong f^{(\alpha_C - 1)} = f^{\epsilon_C/1000} \quad (1)$$

and in the case of hydrogen isotopes

$$\frac{R}{R_0} = \frac{(1000 + \delta^{2}H)}{(1000 + \delta^{2}H_0)} = \frac{(1000 + \delta^{2}H_0 + \Delta\delta^{2}H_{bulk})}{(1000 + \delta^{2}H_0)} \cong f^{(\alpha_H - 1)} = f^{\epsilon_H/1000} \quad (2)$$

where R and R_0 are the average isotope ratios of all MTBE molecules at a given time and at the beginning of the reaction, respectively, and f is the fraction of contaminant remaining at that time. $\delta^{13}C = (R/R_{VPDB} - 1) \times 1000$ is the bulk isotope ratio expressed in the ‰ notation relative to the international carbon standard V−PDB, whereas values of $\delta^2H = (R/R_{VSMOW} - 1) \times 1000$ are expressed with respect to the hydrogen standard VSMOW. $\Delta\delta^{13}C_{bulk} = \delta^{13}C - \delta^{13}C_0$ and $\Delta\delta^2H_{bulk} = \delta^2H - \delta^2H_0$, respectively, describe the changes of these isotope ratios compared to the beginning of the reaction. Experimental data evaluated according to eqs 1 or 2 give the corresponding bulk fractionation factors α and enrichment factors $\epsilon = 1000\ (\alpha - 1)$, which are a measure of how strongly heavy isotopes become enriched in the average MTBE molecules as the reaction proceeds. In the case of no fractionation α is 1 and $\epsilon = 0$‰. The smaller α and the more negative ϵ, the stronger are changes in bulk isotope ratios for a certain degree of conversion, and the more sensitive is the use of CSIA to assess contaminant transformation at contaminated sites. Changes in isotope ratios, for example $\Delta\delta^{13}C_{bulk}$, may then be used to quantitatively estimate the extent of biotic or abiotic degradation in the field, in short biodegradation B, according to the expression

$$B = (1 - f) = 1 - \left[\frac{1000 + \delta^{13}C_0 + \Delta\delta^{13}C_{bulk}}{1000 + \delta^{13}C_0}\right]^{1000/\epsilon} \quad (3)$$

where $\delta^{13}C_0$ is the contaminant isotope ratio at the source and $\Delta\delta^{13}C_{bulk}$ is the change in ratios at some distance away (*24*, *25*).

For such an approach, it is clearly of great importance that values of ϵ be robust and reproducible, as otherwise estimates of B would be associated with considerable uncertainties. In aerobic biodegradation of MTBE, Hunkeler et al. (*23*) and Gray et al. (*22*) measured relatively constrained bulk isotopic enrichment factors ϵ_C between −1.5‰ and −2.5‰ for carbon, and Gray et al. (*22*) determined ϵ_H-values between −29‰ and −66‰ for hydrogen. In contrast, very different results were obtained in the case of anaerobic biodegradation of MTBE. Here, Kolhatkar et al. (*26*), Kuder et al. (*27*, *28*), and Somsamak et al. (*29*, *30*) determined much greater carbon enrichment factors ϵ_C between −9.2‰ and −15.6‰, and Kuder et al. (*27*, *28*) measured significantly smaller hydrogen enrichment factors ϵ_C between −11‰ and −21‰. It is important to understand such systematic variations. On the one hand, the value of ϵ needs to be constrained to be used as the basis for quantification in the field. On the other hand, such isotope patterns reveal important information about biotransformation reaction mechanisms.

At natural abundance, the isotopes are present in all molecular positions. However, because only the molecules with heavy isotopes in the reactive position(s) fractionate (see above), kinetic isotope effects are diluted in the observable average (= "bulk") isotope fractionation that is measurable by GC-IRMS. An adequate analysis was provided by Zwank et al. (*31*) and Elsner et al. (*8*), who corrected for the dilution by non-fractionating molecules and evaluated observable bulk isotope fractionation with respect to position-specific kinetic isotope effects

$$KIE = \frac{^{light}k}{^{heavy}k} \quad (4)$$

where $^{light}k$ and $^{heavy}k$ are the rate constants of molecules containing the light and the heavy isotope in the reacting position. Comparison with literature values showed that the strong hydrogen and weaker carbon isotope fractionation in aerobic MTBE biodegradation matches well the mechanistic model of initial methyl (H_3C-O) group oxidation. In contrast, the strong carbon and relatively weak hydrogen isotope fractionation in anaerobic degradation suggested an initial hydrolysis step via an S_N2 mechanism at the H_3C-O group (*8*).

In addition to oxidation and S_N2 reaction, acid-catalyzed S_N1 hydrolysis has been proposed as a third possible MTBE degradation mechanism (*32*). Small primary carbon and secondary hydrogen isotope effects are predicted for this reaction (*8*). Unlike the other two pathways, however, this mechanism involves the large *tert*-butyl group $(H_3C)_3-C-O$ rather than the small methyl (H_3C-O) group. More relevant atoms are, therefore, located in proximity to the reacting bond, and position-specific KIEs may be more strongly represented in the observable bulk fractionation. It has therefore been postulated that the relative pattern of carbon and hydrogen fractionation may be similar to that of aerobic degradation through oxidation, even though the actual KIE values are smaller and a C−H bond is not even broken in this reaction (*31*). Experimental data to test this hypothesis and to provide isotopic enrichment factors that may serve as reference values for fractionation associated with S_N1 hydrolysis have been lacking to date.

An additional knowledge gap exists for fractionation in aerobic degradation by selective oxidation at the methyl (H_3C-O) group. Although the position-specific kinetic isotope effects for hydrogen (1.7 and 2.5) calculated from data of Gray et al. ($\epsilon_H = -29$‰ and −66‰, (*22*)) are consistent with primary isotope effects as expected for this reaction, they are relatively small compared to the numbers generally reported for C−H bond cleavage ($KIE_H = 3-8$, up to 50 (*8*)). Additional rate-limiting steps other than the strongly fractionating C−H bond cleavage may mask the intrinsic kinetic isotope effect KIE_H so that a smaller apparent kinetic isotope effect (termed $AKIE_H$), and smaller values of ϵ_H are observed. For a systematic investigation, a model reaction that mimics the specific oxidation at the methyl (H_3C-O) group of MTBE but has no preceding slow steps would be helpful. Permanganate is interesting in this respect, as it is reported to perform selective oxidation of C−H bonds next to an ether group (*33*), whereas Fenton's reagent is known to oxidize C−H bonds in a nonselective fashion (*34*).

This research communication addresses the isotope fractionation in abiotic reactions of MTBE transformation. For the first time, carbon and hydrogen isotope fractionation were measured in acid hydrolysis of MTBE and the results were compared to reported data for aerobic and anaerobic (bio)degradation. In addition, this study tested whether permanganate oxidizes MTBE selectively at the methyl (H_3C-O) group. Associated changes in isotope ratios were measured for this reaction in order to constrain the maximum isotope fractionation that can be expected in aerobic biodegradation. As we expect most pronounced changes for hydrogen, we emphasized this element rather than carbon in our inves-

SCHEME 1. Different Reaction Mechanisms of MTBE Degradation

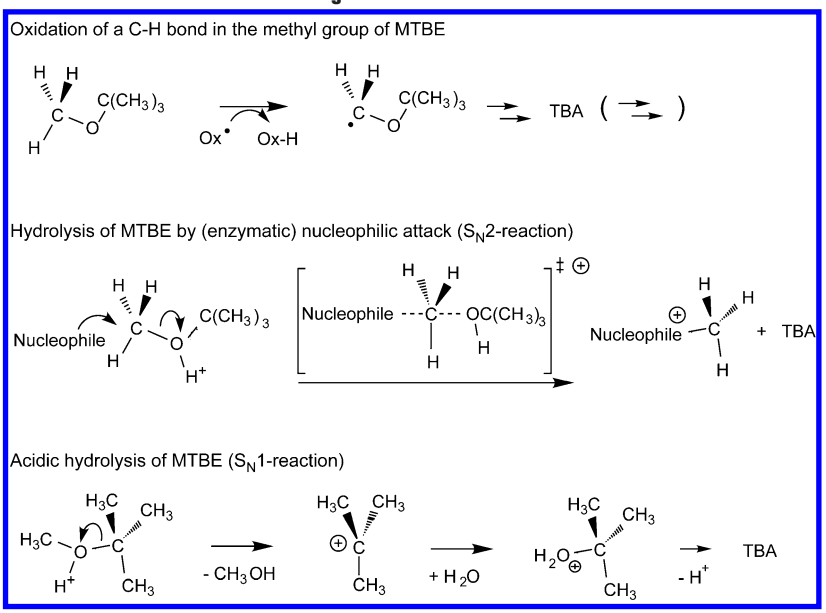

tigation. Observable bulk fractionation is interpreted in the context of a mechanistic understanding using position-specific kinetic isotope effects.

Materials and Methods

A detailed description of the transformation experiments and analytical methods is given in the Supporting Information. Briefly, acid hydrolysis was conducted in the presence of 1200 ppm MTBE and 2 M HCl. Oxidation by permanganate was investigated in solutions containing 1200 ppm MTBE in 0.2 M $KMnO_4$, and 280 ppm di *tert*-butyl ether in 0.2 M $KMnO_4$, respectively. Headspace samples were taken for concentration and isotope analysis. Compound concentrations were measured on a gas chromatograph with flame ionization detector. Hydrogen isotope analysis was conducted on a GC-IRMS (HP 6890 GC, FinniganMATDelta+ XL) interfaced with a micropyrolysis furnace (1440 °C), whereas carbon isotopes were analyzed on a GC-IRMS (Varian 3400 GC, Finnigan MAT 252) equipped with combustion interface. Before isotope analysis, reaction aliquots of the acid hydrolysis were quenched in 2.5 M NaOH. Total uncertainty incorporating both accuracy and reproducibility was ±0.5‰ with respect to V−PDB for carbon isotope analysis and ±5‰ with respect to V−SMOW for hydrogen isotope analysis (*22*).

Regression Analysis. Isotopic enrichment factors were calculated from linear regressions on the logarithmic forms of eqs 1 and 2, rate constants were determined from plots of $\ln(C/C_0)$ versus time, and slopes of $\Delta\delta^2H_{bulk}$ versus $\Delta\delta^{13}C_{bulk}$ were obtained from regression of the original experimental data. Different measures of uncertainty were compared: (a) the standard deviation associated with the slope of the respective linear regression; (b) the total error of the slope calculated by propagation of the known total errors (±5% in the concentration measurements, ±0.5‰ for carbon, and ±5‰ for hydrogen isotope analysis); and (c) the 95% confidence interval on the slope of the regression as obtained from Microsoft Excel using the function "Data Analysis" from the Add-In "Analysis Tool Pack". Standard deviations (a) were about half as large as calculated total errors (b), and these values were still 30% smaller than 95% confidence intervals (c). An exemplary case is discussed in the Supporting Information. In this study we, therefore, consistently report 95% confidence intervals as the largest of the three calculated errors.

Results and Discussion

Acid Hydrolysis. In the presence of 2 M HCl, MTBE was hydrolyzed with a half-life of 1.9 days ($k_{obs} = 0.364 \pm 0.017$ d^{-1}) corresponding to a second-order rate constant of $k = 0.182 \pm 0.009$ d^{-1} M^{-1} (see Figure S1). This is in good agreement with the value of 0.2 h^{-1} M^{-1} reported by O'Reilly et al. (*32*). Methanol and *tert* butanol were the only products detected. Pronounced isotope fractionation was observed for both carbon and hydrogen isotope ratios, corresponding to shifts in bulk isotope ratios of $\Delta\delta^{13}C = -8.5‰ \pm 1‰$ and $\Delta\delta^2H = -91‰ \pm 10‰$ after 88% of conversion. Evaluation of experimental data according to the Rayleigh equation (eqs 1 and 2) resulted in bulk enrichment factors of $\epsilon_C = -4.9‰ \pm 0.6‰$ and $\epsilon_H = -55‰ \pm 7‰$ (Figure 1 a and b). In the case of carbon this is about half as pronounced as in anaerobic (S_N2-type) degradation and twice as much as reported for aerobic methyl group oxidation. For hydrogen, the value is comparable to the number reported for aerobic degradation, which is remarkable considering that no C−H bond is broken in an S_N1 reaction and, therefore, no primary hydrogen isotope effect would be expected (see Scheme 1). The results may be understood, however, if the interplay of primary and secondary isotope effects is considered in the context of reactive positions.

Interpretation of Isotope Fractionation in Terms of Kinetic Isotope Effects. To correct for molecules that carry heavy isotopes in nonreacting positions and are not discriminated against during a reaction, changes in bulk isotope ratios need to be converted into position-specific changes (*8*). As shown in Scheme 1, out of five carbon atoms, only the central position in the *tert*-butyl group reacts so that shifts in bulk isotope ratios $\Delta\delta^{13}C$ need to be multiplied by the factor 5/1:

$$\frac{R_{\text{reactive position}}}{R_{0,\text{reactive position}}} = \frac{(1000 + \delta^{13}C_0 + 5/1 \times \Delta\delta^{13}C_{bulk})}{(1000 + \delta^{13}C_0)} \cong f^{(\alpha_{C,\text{ reactive position}}-1)} = f^{(\epsilon_{C,\text{ reactive position}})/1000} \quad (5)$$

Figure 1c shows the appropriate regression, which yields a position-specific enrichment factor of $\epsilon_{C,\text{reactive position}} =$

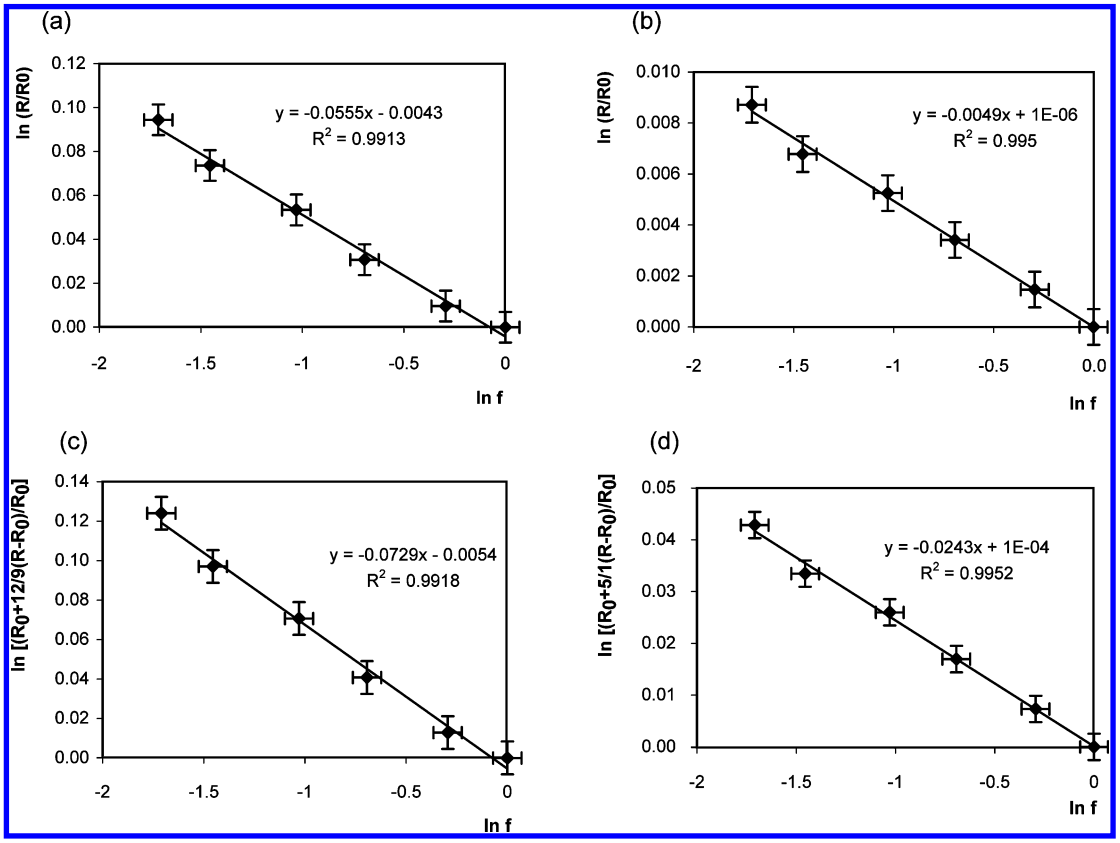

FIGURE 1. Rayleigh plots for isotope fractionation in acid hydrolysis of MTBE: (a) bulk hydrogen isotope fractionation; (b) bulk carbon isotope fractionation; (c) position-specific hydrogen isotope fractionation for the nine hydrogen atoms in the *tert*-butyl group according to eq 7; (d) position-specific carbon isotope fractionation for the central atom in the *tert*-butyl group according to eq 5 .

−24.3‰ ± 2.3‰, corresponding to a kinetic isotope effect calculated after the method of (*8*)

$$\mathrm{KIE_C} = \frac{1}{(1 + \epsilon_{\mathrm{C,reactive\ position}})/1000} = 1.025 \pm 0.003 \quad (6)$$

This number lies in the upper range of values expected for an S_N1 reaction (1.00−1.03), possibly because secondary effects from the other three carbon atoms of the *tert*-butyl group also contributed to the overall fractionation.

In the case of hydrogen, there is no primary isotope effect expected, but secondary isotope effects may be anticipated for the nine hydrogen positions of the *tert*-butyl group. Hence, shifts in bulk isotope ratios $\Delta\delta^2$H are multiplied by the factor 12/9:

$$\frac{R_{\mathrm{reactive\ position}}}{R_{0,\mathrm{reactive\ position}}} = \frac{(1000 + \delta^2\mathrm{H_0} + 12/9 \times \Delta\delta^2\mathrm{H_{bulk}})}{(1000 + \delta^2\mathrm{H_0})} \cong f^{(\alpha_{\mathrm{H,reactive\ position}}-1)} = f^{(\epsilon_{\mathrm{H,reactive\ position}})/1000} \quad (7)$$

The appropriate regression is shown in Figure 1d yielding a position-specific value of $\epsilon_{\mathrm{H,reactive\ position}} = -73‰ \pm 9‰$. Because stabilization of the carbenium ion affects all nine hydrogen atoms in the same way, there is no intramolecular competition between them, and the corresponding secondary kinetic isotope effect can be calculated after the method of (*8*)

$$\mathrm{KIE_H} = \frac{1}{1 + \epsilon_{\mathrm{H,reactive\ position}}/1000} = 1.08 \pm 0.01 \quad (8)$$

which is in agreement with $\mathrm{KIE_H}$ values of 1.05−1.15 reported for such a reaction (*8*).

Overall, measured carbon and hydrogen isotope fractionation during MTBE acid hydrolysis are, therefore, consistent with the proposed mechanistic model. This is also demonstrated by the ratio of the position-specific enrichment factors $\epsilon_{\mathrm{reactive\ position,H}}/\epsilon_{\mathrm{reactive\ position,C}} = 3.0 \pm 0.7$, which is consistent with the range of 1.6 to ∞ predicted from the following equation (eq 23 in (*8*)):

$$\frac{\epsilon_{\mathrm{reactive\ position,H}}}{\epsilon_{\mathrm{reactive\ position,C}}} \approx \frac{(\alpha_{\mathrm{reactive\ position,H}})^{-1} - 1}{(\alpha_{\mathrm{reactive\ position,C}})^{-1} - 1} = \frac{\mathrm{KIE_H} - 1}{\mathrm{KIE_C} - 1} \times \frac{1 + \mathrm{KIE_C} \times (z_\mathrm{C} - 1)}{1 + \mathrm{KIE_H} \times (z_\mathrm{H} - 1)} \quad (9)$$

A derivation of the approximate equivalence of $\epsilon_{\mathrm{rp,H}}/\epsilon_{\mathrm{rp,C}}$ and $((\alpha_{\mathrm{rp,\,H}})^{-1} - 1)/((\alpha_{\mathrm{rp,\,C}})^{-1} - 1)$ is provided in the Supporting Information.

Reaction Mechanisms from Isotope Plots of Two Elements. For the interpretation of data from samples for which the degradation mechanism is unknown, it is of great interest to determine whether the relative changes in isotope ratios of the two elements, $\Delta\delta^2\mathrm{H_{bulk}}/\Delta\delta^{13}\mathrm{C_{bulk}}$, are sufficiently distinct to distinguish between S_N1-type hydrolysis, aerobic degradation through methyl group oxidation, and anaerobic biodegradation by an S_N2-type hydrolysis. Figure 2 shows the data of the present study together with data of previous studies measuring isotopic fractionation during anaerobic (*28*) and aerobic biodegradation (*22*). The corresponding slopes of $\Delta\delta^2\mathrm{H_{bulk}}/\Delta\delta^{13}\mathrm{C_{bulk}}$ are 11.1 ± 1.3 (S_N1-type hydrolysis), 17.8 ± 3.4 (methyl group oxidation), and 1.2 ± 0.8 (S_N2-type hydrolysis), where the given errors are 95% confidence intervals obtained on the slope of the linear

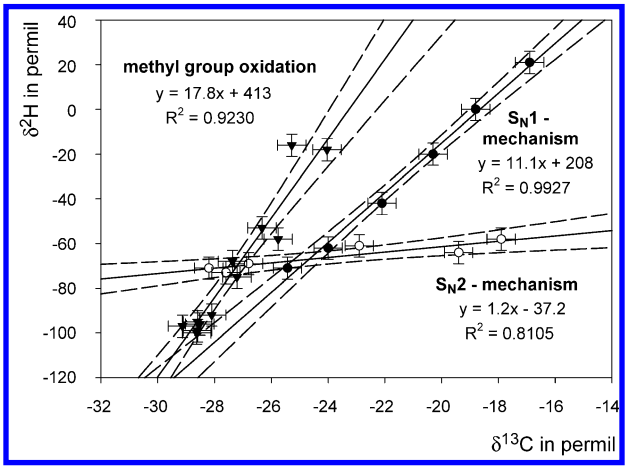

FIGURE 2. Changes in carbon and hydrogen isotope ratios for degradation of MTBE by different mechanisms. The two-dimensional plot includes data from this study for acid hydrolysis via an S_N1 mechanism (●), data from Kuder et al. (*28*) for anaerobic biodegradation via an S_N2 mechanism (○), and data from Gray et al. (*22*) for aerobic biodegradation via methyl group oxidation (▼). Dashed lines indicate 95% confidence intervals of the respective regressions.

regression. For the case of acid hydrolysis, the result illustrates that $\Delta\delta^2H_{bulk}/\Delta\delta^{13}C_{bulk}$, $\epsilon_{bulk,H}/\epsilon_{bulk,C}$, and $\epsilon_{reactive\ position,H}/\epsilon_{reactive\ position,C}$ are approximately related according to

$$\frac{\Delta\delta^2H_{bulk}}{\Delta\delta^{13}C_{bulk}} = 11.1$$

$$\approx \frac{\epsilon_{bulk,H}}{\epsilon_{bulk,C}} = \frac{-55‰}{-4.9‰} = 11.2$$

$$\approx \frac{9/12 \times \epsilon_{reactive\ position,H}}{1/5 \times \epsilon_{reactive\ position,C}} = \frac{9/12 \times (-73‰)}{1/5 \times (-24.3‰)} = 11.3 \quad (10)$$

so that slopes of two-dimensional isotope plots may in principle be predicted from eq 9. As mentioned in the introduction, while this approach could indeed unequivocally establish characteristic trends for aerobic methyl group oxidation and anaerobic S_N2-type hydrolysis (*8*), it has not been possible, however, to predict from theory whether significantly different trends would be expected between oxidation and S_N1-type hydrolysis (*31*). As illustrated in Figure 2, the actual experimental data for acid hydrolysis now demonstrate that significant differences do exist among the three reactions and suggests that trends in $\Delta\delta^2H_{bulk}/\Delta\delta^{13}C_{bulk}$ have the potential to discern among degradation mechanisms in natural systems as well. Figure 2 indicates that at least 50% conversion is necessary, however, to distinguish between methyl oxidation and S_N1-type hydrolysis, whereas the S_N2-mechanism can be discerned already at early stages of degradation.

Permanganate Oxidation. Oxidation of MTBE in the presence of 0.2 M permanganate was rapid with a half-life of 0.76 days ($k_{obs} = 0.91 \pm 0.03\ d^{-1}$) corresponding to a second-order rate constant of $k = 4.6 \pm 0.2\ d^{-1}\ M^{-1}$ (see Figure S2). This value is in good agreement with Damm et al. (*35*) who reported a k value of $1.6\ 10^{-6}\ h^{-1}\ mg^{-1}$ L, corresponding to $4.1\ d^{-1}\ M^{-1}$. The selectivity of the oxidation was tested by investigating the reactivity of di-*tert*-butyl ether in the presence of 0.2 M permanganate over 7 days. No significant conversion was observed during that time (see Figure S3), demonstrating that the C−H bonds in the *tert*-butyl groups were inert during oxidation by permanganate. It can therefore be concluded that the *tert*-butyl group in MTBE was not reactive either under these conditions and that transformation of MTBE occurred entirely through oxidation at the methyl group. Scheme 2 shows the reaction in analogy to the mechanism proposed for permanganate oxidation of toluene in water (*36*).

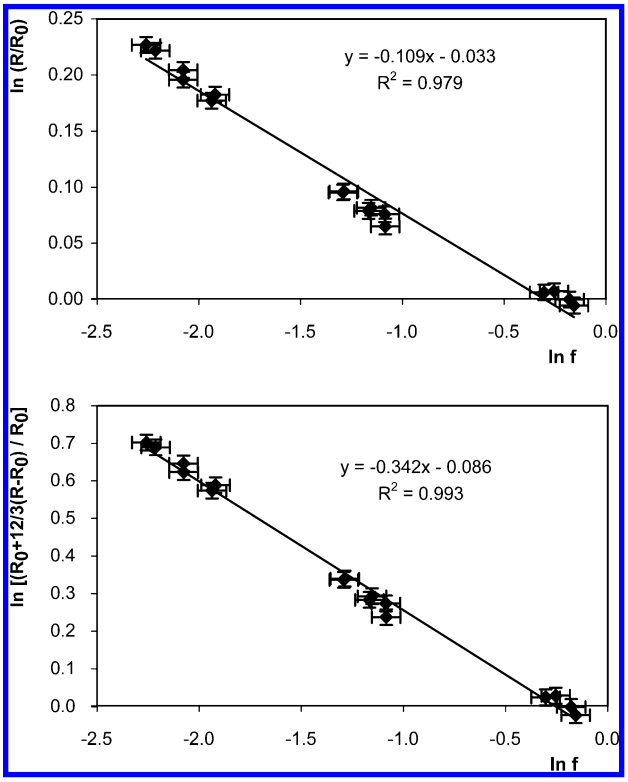

FIGURE 3. Rayleigh plots for hydrogen isotope fractionation in oxidation of MTBE by permanganate: (a) bulk isotope fractionation; (b) position-specific isotope fractionation for the three hydrogen atoms in the methyl group according to eq 11.

Hydrogen Isotope Fractionation. Pronounced hydrogen isotope fractionation was observed during oxidation of MTBE by permanganate, with isotope ratios of δ^2H changing from values of $-65‰ \pm 5‰$ to values as enriched as $\delta^2H = +175‰ \pm 5‰$ after 90% of conversion. Carbon isotope fractionation was not analyzed in this experiment. As shown in Figure 3a, evaluation of hydrogen bulk isotope data according to eq 2 resulted in a remarkably large bulk enrichment factor of $\epsilon_H = -109‰ \pm 9‰$ with $R^2 = 0.979$. The corresponding position-specific enrichment factor was calculated by considering that only 3 out of 12 total hydrogen atoms were located in the reacting methyl group such that

$$\frac{R_{reactive\ position}}{R_{0,reactive\ position}} = \frac{(1000 + \delta^2H_0 + 12/3 \times \Delta\delta^2H_{bulk})}{(1000 + \delta^2H_0)} \cong f^{(\alpha_{H,reactive\ position}-1)} = f^{(\epsilon_{H,reactive\ position})/1000} \quad (11)$$

giving $\epsilon_{H,reactive\ position} = -342‰ \pm 16‰$ with an $R^2 = 0.993$ for the corresponding regression shown in Figure 3b. As indicated by the higher R^2 value, the regression was better than in the case of the bulk data in Figure 3a, a phenomenon that has been predicted by Elsner et al. (*8*). Molecules with an ^2H-atom in the methyl group are expected to accumulate preferentially in the remaining substrate compared to molecules with ^2H in the *tert*-butyl group as the reaction proceeds. This enrichment of more strongly fractionating molecules results in nonlinear regressions with a bulk fractionation that becomes larger as more data from late time points are included. Correction for nonreacting positions

SCHEME 2. Methyl Group Oxidation by Permanganate

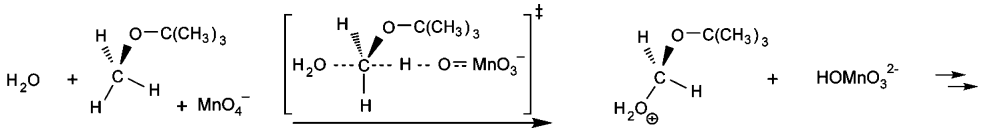

according to eq 11 serves to eliminate this artifact. The data of this study illustrate that inadequate results may indeed be obtained if values of $\epsilon_{H,reactive\ position}$ are calculated according to the following approximate equation (eq 16 in (*8*))

$$\epsilon_{reactive\ position} \approx 12/3 \times \epsilon_{bulk} \quad (12)$$

giving in the current example a number of −436‰ ± 36‰ instead of the value of −342‰ ± 16‰ calculated above.

Interpretation in Terms of Kinetic Isotope Effects. The significance of this difference becomes evident if values of $\epsilon_{H,reactive\ position}$ are used to calculate position-specific kinetic isotope effects according to

$$\frac{\epsilon_{H,reactive\ position}}{1000} + 1 = \alpha_{H,reactive\ position} = \frac{1 \times {}^{2}k + 2 \times {}^{1}k_{next\ to\ a\ deuterium-containing\ bond}}{3 \times {}^{1}k} = \frac{1}{3} \times KIE_{H,primary}{}^{-1} + \frac{2}{3} \times KIE_{H,secondary}{}^{-1} \quad (13)$$

This equation takes into account that at natural isotopic abundance only one ^{2}H atom is present in the methyl group. Only in one-third of all cases is therefore ^{2}H in the reacting bond causing a primary isotope effect, while in two-thirds it is next to the reacting bond causing a secondary isotope effect. Such secondary effects may often be neglected giving approximately

$$\frac{\epsilon_{H,reactive\ position}}{1000} + 1 \approx \frac{1}{3} \times KIE_{H,primary}{}^{-1} + \frac{2}{3} \Leftrightarrow KIE_{H,primary} \approx \frac{1}{3 \times (\epsilon_{H,reactive\ position})/1000 + 1} \quad (14)$$

With this approximation, it is evident that $\epsilon_{H,reactive\ position}$ = −333‰ is the most negative number to be expected for a methyl group, as otherwise calculated KIE_H numbers would become negative. The $\epsilon_{H,\ reactive\ position}$ = −342‰ ± 16‰ of this study slightly exceeds this limit but may be rationalized if, in addition, also secondary effects are taken into account according to eq 13. Possible combinations resulting in $\epsilon_{H,reactive\ position}$ = −342‰ are, for example $KIE_{H,primary}$ = 6.4, $KIE_{H,secondary}$ = 1.1; $KIE_{H,primary}$ = 3.3, $KIE_{H,secondary}$ = 1.2; $KIE_{H,primary}$ = 2.3, $KIE_{H,secondary}$ = 1.3, see Supporting Information. In contrast, the value of $\epsilon_{H,reactive\ position}$ = −436‰ ± 36‰ that is obtained from eq 12 is difficult to explain, and the following approximate equation (eq 22 in (*8*))

$$KIE_H \approx \frac{1}{1 + 12 \times \epsilon_{H,bulk}/1000} \quad (15)$$

does not lead to any meaningful results in such cases of large hydrogen isotope fractionation. We note, however, that the effects discussed here are mainly relevant in cases of strong fractionation such as with hydrogen and may in good approximation be neglected with other elements, for which eq 15 generally gives good results (*8*).

Masking in Aerobic Biodegradation. The results of the present study demonstrate that position-specific enrichment factors $\epsilon_{H,reactive\ position}$ of up to −342‰ may be expected for methyl group oxidation. Although the actual reaction mechanism is not the same as proposed for most monooxygenases (see Scheme 1 vs 2), kinetic isotope effects calculated according to eq 13 are well comparable with the large values that are typically determined with such enzymes (*37*). This indicates that the number of around −342‰ may serve as a tentative benchmark also for biotransformation of MTBE, provided that the enzymatic C−H bond cleavage in aerobic biotransformation is rate determining. Evaluation of original data of Gray et al. (*22*) in ref *8*, however, resulted in much smaller values of $\epsilon_{H,reactive\ position}$ between −136‰ and −204‰, suggesting additional rate-limiting reaction steps prior to or in the biochemical transformation. The following equation of Northrop (*38*) has been derived to describe the relationship of apparent (AKIE) and intrinsic (KIE) isotope effects in experiments with labeled substrate

$$AKIE_{labeled\ substrate} = \frac{C + KIE}{C + 1} \quad (16)$$

Here, the term *C*, called commitment to catalysis, describes how fast the actual C−H bond cleavage is compared to all steps that lead back to free substrate. If *C* is large, the C−H bond is broken quickly and the reverse reaction in the preceding steps is slow. Because few molecules get back to the original substrate pool—irrespective of their isotopic composition—the intrinsic discrimination cannot be observed and AKIE values are much smaller than the intrinsic KIE numbers. In Part S4 of the Supporting Information, values of *C* between 1 and 2.3 are estimated based on the assumption that intrinsic position-specific enrichment factors in aerobic biodegradation of MTBE are the same as for abiotic oxidation (−342‰). Even in the case of relatively pronounced hydrogen fractionation as observed by Gray et al. (*22*), preceding steps in the biochemical transformation were, therefore, already equally slow or even by a factor of 2.3 slower than the actual bond cleavage. As masking affects carbon isotope fractionation in the same way, such effects clearly need to be considered if enrichment factors are chosen for quantifying natural biodegradation according to eq 3. There are a limited number of hydrogen enrichment factors ϵ_H available in the literature and the results of this study show that ϵ_H associated with aerobic biodegradation have the potential to be as large as −109‰, whereas the largest value measured to date is just −66‰. For conservative estimates of the effects of biodegradation, the use of largest reported values is, therefore, recommended.

Environmental Significance

Three fundamentally different mechanisms have been proposed for degradation of MTBE: S_N1-type hydrolysis, aerobic degradation through methyl group oxidation, and anaerobic biodegradation by an S_N2-type hydrolysis. This study demonstrates that each of these mechanisms have a distinct relationship of carbon versus hydrogen fractionation, highlighting the potential to distinguish between the different mechanisms at contaminated field sites by plotting isotope data of $\Delta\delta^2H_{bulk}/\Delta\delta^{13}C_{bulk}$ in two-dimensional diagrams (Figure 2). At contaminated sites, such a procedure would assist in the selection of the appropriate bulk enrichment factor ϵ_{bulk} for quantification of the extent of natural biodegradation using eq 3. Care must be taken, however, to under- rather than overestimate natural attenuation in order to obtain conservative estimates. This study illustrates that reported bulk enrichment factors of MTBE not only reflect

the intrinsic fractionation of the biochemical transformation, but may also be affected by the presence of additional rate-limiting steps in the overall biodegradation. Similar effects have been reported for biotransformation of chlorinated ethenes (*39*) and toluene (*40*). As discussed above, for quantification of biodegradation according to eq 3, it is therefore recommended to use the largest value of ϵ_{bulk} within a reported range.

Acknowledgments

This work was supported by the German Research Foundation (DFG) Research Fellowship 266/1-3 to M.E., and by the NSERC Strategic Grants Program and Discovery Program. We thank three anonymous reviewers for helpful comments that improved the quality of the manuscript.

Supporting Information Available

S1. Methods and Materials; S2. Exemplary regression analysis; S3. Derivation of the approximate equivalence of $\epsilon_{rp,H}/\epsilon_{rp,C}$ and $((\alpha_{rp,H})^{-1} - 1)/((\alpha_{rp,C})^{-1} - 1)$ in eq 9; S4. Possible combinations of primary and secondary KIE_H resulting in $\epsilon_{H,\text{reactive position}} = -342‰$; S5. Tentative calculation of *C* (commitment to catalysis) values for reported biotransformation of MTBE; Figures S1, S2: Regression on concentration/time data in acid hydrolysis of MTBE and in oxidation by permanganate; Figure S3: Reactivity of di *tert*-butyl ether over time in the presence of 0.2 M permanganate. This material is available free of charge via the Internet at http://pubs.acs.org.

Literature Cited

(1) Krayer von Krauss, M., Harremoes, P., Eds. *MTBE in Petrol as Substitute for Lead*; Office for Official Publications of the European Communities: Copenhagen, 2001.

(2) Moran, M. J.; Zogorski, J. S.; Squillace, P. J. MTBE and gasoline hydrocarbons in ground water of the United States. *Ground Water* **2005**, *43*, 615−627.

(3) Schmidt, T. C.; Duong, H. A.; Berg, M.; Haderlein, S. B. Analysis of fuel oxygenates in the environment. *Analyst* **2001**, *126*, 405−413.

(4) Squillace, P. J.; Pankow, J. F.; Korte, N. E.; Zogorski, J. S. Review of the environmental behavior and fate of methyl tert-butyl ether. *Environ. Toxicol. Chem.* **1997**, *16*, 1836−1844.

(5) Schirmer, M.; Barker, J. F. A study of long-term MTBE attenuation in the borden aquifer, Ontario, Canada. *Ground Water Monit. Rem.* **1998**, *18*, 113−122.

(6) Schmidt, T. C.; Schirmer, M.; Weiss, H.; Haderlein, S. B. Microbial degradation of methyl tert-butyl ether and tert-butyl alcohol in the subsurface. *J. Contam. Hydrol.* **2004**, *70*, 173−203.

(7) Wilson, J. T.; Kaiser, P. M.; Adair, C. *Monitored Natural Attenuation of MTBE as a Risk Management Option at Leaking Underground Storage Tank Sites*; U.S. EPA: Cincinnati, OH, 2005.

(8) Elsner, M.; Zwank, L.; Hunkeler, D.; Schwarzenbach, R. P. A new concept linking observable stable isotope fractionation to transformation pathways of organic pollutants. *Environ. Sci. Technol.* **2005**, *39*, 6896−6916.

(9) Harrington, R. R.; Poulson, S. R.; Drever, J. I.; Colberg, P. J. S.; Kelly, E. F. Carbon isotope systematics of monoaromatic hydrocarbons: vaporization and adsorption experiments. *Org. Geochem.* **1999**, *30*, 765−775.

(10) Ward, J. A. M.; Ahad, J. M. E.; Lacrampe-Couloume, G.; Slater, G. F.; Edwards, E. A.; Sherwood, Lollar, B. Hydrogen isotope fractionation during methanogenic degradation of toluene: potential for direct verification of bioremediation. *Environ. Sci. Technol.* **2000**, *34*, 4577−4581.

(11) Haderlein, S. B.; Schmidt, T. C.; Elsner, M.; Zwank, L.; Berg, M.; Schwarzenbach, R. P. Response to comment on "New evaluation scheme for two-dimensional isotope analysis to decipher biodegradation processes: Application to groundwater contamination by MTBE". *Environ. Sci. Technol.* **2005**, *39*, 8543−8544.

(12) Dempster, H. S.; Sherwood Lollar, B.; Feenstra, S. Tracing organic contaminants in groundwater: A new methodology using compound specific isotopic analysis. *Environ. Sci. Technol.* **1997**, *31*, 3193−3197.

(13) Slater, G. F.; Dempster, H. S.; Sherwood Lollar, B.; Ahad, J. Headspace analysis: a new application for isotopic characterization of dissolved organic contaminants. *J. Contam. Hydrol.* **1999**, *33*, 190−194.

(14) Hunkeler, D.; Chollet, N.; Pittet, X.; Aravena, R.; Cherry, J. A.; Parker, B. L. Effect of source variability and transport processes on carbon isotope ratios of TCE and PCE in two sandy aquifers. *J. Contam. Hydrol.* **2004**, *74*, 265−282.

(15) Bouchard, D. Use of stable isotope analysis to assess biodegradation of volatile organic compounds in the unsaturated zone. Ph.D. Thesis, University of Neuchâtel, Neuchâtel, 2007.

(16) Slater, G. F.; Ahad, J. M. E.; Sherwood Lollar, B.; Allen-King, R.; Sleep, B. Carbon isotope effects resulting from equilibrium sorption of dissolved VOCs. *Anal. Chem.* **2000**, *72*, 5669−5672.

(17) Meckenstock, R. U.; Morasch, B.; Warthmann, R.; Schink, B.; Annweiler, E.; Michaelis, W.; Richnow, H. H. $^{13}C/^{12}C$ isotope fractionation of aromatic hydrocarbons during microbial degradation. *Environ. Microbiol.* **1999**, *1*, 409−414.

(18) Schuth, C.; Taubald, H.; Bolano, N.; Maciejczyk, K. Carbon and hydrogen isotope effects during sorption of organic contaminants on carbonaceous materials. *J. Contam. Hydrol.* **2003**, *64*, 269−281.

(19) Kopinke, F. D.; Georgi, A.; Voskamp, M.; Richnow, H. H. Carbon isotope fractionation of organic contaminants due to retardation on humic substances: Implications for natural attenuation studies in aquifers. *Environ. Sci. Technol.* **2005**, *39*, 6052−6062.

(20) Wang, Y.; Huang, Y. Hydrogen isotopic fractionation of petroleum hydrocarbons during vaporization: implications for assessing artificial and natural remediation of petroleum contamination. *Org. Geochem.* **2003**, *18*, 1641−1651.

(21) Prinzhofer, A.; Pernaton, E. Isotopically light methane in natural gas: bacterial imprint or diffusive fractionation. *Chem. Geol.* **1997**, *142*, 193−200.

(22) Gray, J. R.; Lacrampe-Couloume, G.; Gandhi, D.; Scow, K. M.; Wilson, R. D.; Mackay, D. M.; Sherwood Lollar, B. Carbon and hydrogen isotopic fractionation during biodegradation of methyl *tert*-butyl ether. *Environ. Sci. Technol.* **2002**, *36*, 1931−1938.

(23) Hunkeler, D.; Butler, B. J.; Aravena, R.; Barker, J. F. Monitoring biodegradation of methyl tert-butyl ether (MTBE) using compound-specific carbon isotope analysis. *Environ. Sci. Technol.* **2001**, *35*, 676−681.

(24) Sherwood Lollar, B.; Slater, G. F.; Sleep, B.; Witt, M.; Klecka, G. M.; Harkness, M.; Spivack, J. Stable carbon isotope evidence for intrinsic bioremediation of tetrachloroethene and trichloroethene at Area 6, Dover Air Force Base. *Environ. Sci. Technol.* **2001**, *35*, 261−269.

(25) Meckenstock, R. U.; Morasch, B.; Griebler, C.; Richnow, H. H. Stable isotope fractionation analysis as a tool to monitor biodegradation in contaminated acquifers. *J. Contam. Hydrol.* **2004**, *75*, 215−255.

(26) Kolhatkar, R.; Kuder, T.; Philip, P.; Allen, J.; Wilson, J. T. Use of compound-specific stable carbon isotope analyses to demonstrate anaerobic biodegradation of MTBE in groundwater at a gasoline release site. *Environ. Sci. Technol.* **2002**, *36*, 5139−5146.

(27) Kuder, T.; Philp, R. P.; Kolhatkar, R.; Wilson, J. T.; Allen, J. Application of stable carbon and hydrogen isotopic techniques for monitoring biodegradation of MTBE in the field. In *NGWA/API Petroleum Hydrocarbons and Organic Chemicals in Ground Water*; American Petroleum Institute: Atlanta, GA, 2002.

(28) Kuder, T.; Wilson, J. T.; Kaiser, P.; Kolhatkar, R.; Philp, P.; Allen, J. Enrichment of stable carbon and hydrogen isotopes during anaerobic biodegradation of MTBE: Microcosm and field evidence. *Environ. Sci. Technol.* **2005**, *39*, 213−220.

(29) Somsamak, P.; Richnow, H. H.; Haggblom, M. M. Carbon isotopic fractionation during anaerobic biotransformation of methyl tert-butyl ether and tert-amyl methyl ether. *Environ. Sci. Technol.* **2005**, *39*, 103−109.

(30) Somsamak, P.; Richnow, H. H.; Haggblom, M. M. Carbon isotope fractionation during anaerobic degradation of methyl *tert*-butyl ether under sulfate-reducing and methanogenic conditions. *Appl. Environ. Microbiol.* **2006**, *72*, 1157−1163.

(31) Zwank, L.; Berg, M.; Elsner, M.; Schmidt, T. C.; Schwarzenbach, R. P.; Haderlein, S. B. New evaluation scheme for two-dimensional isotope analysis to decipher biodegradation processes: Application to groundwater contamination by MTBE. *Environ. Sci. Technol.* **2005**, *39*, 1018−1029.

(32) O'Reilly, K. T.; Moir, M. E.; Taylor, C. D.; Smith, C. A.; Hyman, M. R. Hydrolysis of tert-butyl methyl ether the (MTBE) in dilute aqueous acid. *Environ. Sci. Technol.* **2001**, *35*, 3954−3961.

(33) Schmidt, H.-J.; Schafer, H. J. Oxidation of ethers with benzyl-(triethyl)ammonium permanganate. *Angew. Chem. Int. Ed. Engl.* **1979**, *18*, 69−70.
(34) Xu, X. R.; Zhao, Z. Y.; Li, X. Y.; Gu, J. D. Chemical oxidative degradation of methyl tert-butyl ether in aqueous solution by Fenton's reagent. *Chemosphere* **2004**, *55*, 73−79.
(35) Damm, J. H.; Hardacre, C.; Kalin, R. M.; Walsh, K. P. Kinetics of the oxidation of methyl tert-butyl ether (MTBE) by potassium permanganate. *Water Res.* **2002**, *36*, 3638−3646.
(36) Gardner, K. A.; Mayer, J. M. Understanding C-H bond oxidations: Hdot and H- transfer in the oxidation of toluene by permanganate. *Science* **1995**, *269*, 1849−1851.
(37) Nesheim, J. C.; Lipscomb, J. D. Large kinetic isotope effects in methane oxidation catalyzed by methane monooxygenase: evidence for C-H bond cleavage in a reaction cycle intermediate. *Biochemistry* **1996**, *35*, 10240−10247.
(38) Northrop, D. B. Steady-State Analysis of Kinetic Isotope Effects in Enzymatic Reactions. *Biochemistry* **1975**, *14*, 2644−2651.
(39) Nijenhuis, I.; Andert, J.; Beck, K.; Kastner, M.; Diekert, G.; Richnow, H. H. Stable isotope fractionation of tetrachloroethene during reductive dechlorination by *Sulfurospirillum multivorans* and *Desulfitobacterium* sp. Strain PCE-S and abiotic reactions with cyanocobalamin. *Appl. Environ. Microbiol.* **2005**, *71*, 3413−3419.
(40) Mancini, S. A.; Hirschorn, S. K.; Elsner, M.; Lacrampe-Couloume, G.; Sleep, B. E.; Edwards, E. A.; Sherwood Lollar, B. Effects of Trace Element Concentration on Enzyme Controlled Stable Isotope Fractionation during Aerobic Biodegradation of Toluene. *Environ. Sci. Technol.* **2006**, *40*, 7675−7681.

Received for review March 2, 2007. Revised manuscript received May 29, 2007. Accepted June 3, 2007.

ES070531O